Published in final edited form as:
Dev Dyn. 2010 October ; 239(10): 2748–2760. doi:10.1002/dvdy.22402.

Analysis of a *Hand1* hypomorphic allele reveals a critical threshold for embryonic viability

Beth A. Firulli, **David P. McConville**, **James S. Byers III**, **Joshua W. Vincentz**, **Ralston M. Barnes**, and **Anthony B. Firulli***
Riley Heart Research Center, Herman B Wells Center for Pediatric Research Division of Pediatrics Cardiology, Departments Anatomy and Medical and Molecular Genetics, Indiana Medical School, 1044 W. Walnut St., Indianapolis, IN 46202-5225, USA

Abstract

Loss-of-function analysis of the bHLH transcription factor Hand1 indicates critical roles in development. In an effort to generate a *Hand1* cDNA knock-in reporter mouse, we generated two hypomorphic alleles, which extend embryonic survival to between E10.5 and E12.5. Heart morphogenesis appears largely normal; however, hypomorphic mice display thin left ventricular myocardium and reduction in pharyngeal mesoderm. Caudal defects, large allantois, and thickened yolk sac are observed and consistent with systemic *Hand1* gene deletion. *Hand1* mRNA is expressed at 30% of wild-type littermates and known *Hand1*-dependent genes show intermediate expression compared to wild-type and *Hand1* null mice. Interestingly, putative bHLH partners, *Hand2* and *Twist1*, show altered expression in both *Hand1* null and hypomorphic backgrounds and intercrossing the *Hand1* hypomorphic mice onto the *Hand2* systemic null background exacerbates the cardiac and lateral mesoderm phenotypes. Together, these data define a critical threshold of *Hand1* expression that is necessary for embryonic survival.

Keywords

Hand1; *Hand2*; heart development; ventricle; extraembryonic mesoderm

INTRODUCTION

Members of the Twist-family of basic helix-loop-helix (bHLH) transcription factors perform essential roles in embryonic development and pathological disease (Firulli, 2003; Firulli and Conway, 2008; Barnes and Firulli, 2009). The Twist-family member Hand1 not only plays essential roles in the development of the heart and sympathetic nervous system but also holds an early role in maintaining the viability of the extraembryonic mesoderm that contributes to the placenta, yolk sac, amnion, allantois, vasculature and trophoblast giant cells (Firulli et al., 1998; Riley et al., 1998; Morikawa and Cserjesi, 2004). *Hand1* null mice die between E8.5 to E9.0 resulting from defects in the extraembryonic mesoderm and trophoblast giant cells in the ectoplacental cone (Firulli et al., 1998; Riley et al., 1998). Expression of *Placental Lactogen I* (*Prld* or *Pl1*) is greatly reduced in *Hand1* null embryos (Firulli et al., 1998; Riley et al., 1998). During early mouse gestation (up to E11.0), Pl1 maintains the corpus luteum, the source of progesterone, which is required for successful pregnancy (Walker et al., 1991; Yamaguchi et al., 1994). Vascular formation within the *Hand1* null yolk sac initiates, but soon after, becomes developmentally arrested. Expression of *vascular endothelial growth factor* (*Vegf*), *Angiopoietin (Angpt1)* and *ephrin B2* are

*To whom correspondence should be addressed tfirulli@iupui.edu (317) 278-5814.

subsequently upregulated. Moreover, smooth muscle cells abnormally cluster throughout the yolk sac mesoderm (Morikawa and Cserjesi, 2004). Conditional deletion of *Hand1* has revealed genetic interactions with the related family member *Hand2* (McFadden et al., 2005). *αMHC-Cre* and *Nkx2.5-Cre* mediated cardiac deletion of *Hand1* results in perinatal lethality due to ventricular septal defects and accompanying overriding aorta or double outlet right ventricle (McFadden et al., 2005). Ablating *Hand1* in the heart on a *Hand2* haploinsufficient background increases the severity of these observed phenotypes. Such genetic interactions, in part, manifest due to the broad dimerization affinities of the Twist-family bHLH proteins compared to those of other Class B bHLH factors (Firulli et al., 2003; Firulli and Conway, 2008 Firulli, 2005 #2346). Twist-family proteins can form homodimers and heterodimers with both other Class B bHLH factors and E-proteins. Thus, in gene deletion experiments, phenotypes reflect the loss-of-function as well as a consequent redistribution of the bHLH dimer pool within a cell. It is therefore not surprising that the control of *Hand* and *Twist* gene expression levels is tightly regulated.

In our efforts to generate a *Hand1* maker allele that would not be haploinsufficient for *Hand1*, we employed a cDNA knock-in approach in conjunction with an *IRES-eGFP* cassette to allow for visualization of *Hand1*-expressing cells. Analysis shows that *Hand1* homozygous cDNA knock-in mice are not viable and that the removal of the neomycin cassette does not rescue lethality. Embryonic analysis shows that eGFP epiflorescence was not detectable in heterozygous or homozygous embryos; however, mRNA expression is detectable. Interestingly, homozygous knock-in embryos die between E10–E12.5, exhibiting a clear extension of survival from that observed in the *Hand1* systemic knockouts. Phenotypic analysis reveals thin dilated hearts and dysmorphic caudal development as well as the predicted yolk sac and extra-embryonic phenotypes. Cell death and proliferation analyses reveal that there is no change in apoptosis; however, a global decrease in cell proliferation as a consequence of poor placental function is observed. mRNA analysis shows that the *Hand1* cDNA knock-in alleles are hypomorphic, with expression of *Hand1* at 30%–40% of that observed in wildtype littermates, thus defining a threshold of necessary *Hand1* expression. Accompanying this decrease in *Hand1* expression is an upregulation of *Hand2*, which could be either compensatory or deleterious, resulting in a further destabilization of the bHLH factory stoichiometry. Intercross of the *Hand1* hypomorphic allele onto a *Hand2* null background largely exacerbates these observed phenotypes, indicating the importance of Twist-family gene balance in embryogenesis.

RESULTS

Generation of $Hand1^{Hand1+Neo}$ and $Hand1^{Hand1\Delta Neo}$ cDNA knock-in mice

To follow real-time *Hand1* expression without lowering the *Hand1* gene dosage, we designed a cDNA knock-in approach, whereby the coding region of *Hand1* from a 600bp cDNA initiating at the ATG and terminating at the stop codon was cloned 5′ of an IRES followed by an eGFP expression cassette. The replacement cDNA cassette was flanked by 5′ and 3′ *Hand1* targeting arms that have been described previously (Firulli et al., 1998). ES cells targeted at a frequency of approximately 1:15. Two independent ES cell lines were injected into host blastocysts, which produced chimeric mice that subsequently gave rise to the germline transmission of the of the $Hand1^{Hand1+Neo}$ allele (Fig. 1A). Both ES lines generated mice that exhibit identical phenotypes and thus are considered identical.

Intercross of $Hand1^{Hand1+Neo/+}$ F1 mice produces no homozygous $Hand1^{Hand1+Neo/Hand1+Neo}$ offspring at P10, suggesting that the cDNA allele constructed is not expressing at normal levels. Subsequent eGFP whole mount and section analyses of E9.5 embryos show a lack of detectable epiflorescence; however, both heterozygous and homozygous genotypes were identified. Compared to the systemic mutants, E9.5 *Hand1*

knockout (*Hand1*$^{LacZ/LacZ}$), E9.5 *Hand1*$^{Hand1+Neo/Hand1+Neo}$ embryos are larger, further developed, and had visible heartbeats. Cardiac morphology appeared normal, although hearts appear large compared to overall embryo size. The caudal region of the embryos display crooked neural tubes, overtly large allantoises, and yolks sac blistering resulting from separation of the visceral mesoderm and endoderm of the yolk sac (Fig 1B). These phenotypes are also observed, albeit to a more pronounced degree, in *Hand1*$^{LacZ/LacZ}$ mice, suggesting that the cause of death, consistent with previous findings, is placental insufficiencies (Firulli et al., 1998;Riley et al., 1998). Given that we encountered a less severe phenotype, we extended our analysis to E12.5. We detected viable (displaying regular heart beat) *Hand1*$^{Hand1+Neo/Hand1+Neo}$ embryos at E10.5 but no viable mice were observed after this time point.

To look at the influence of the *PGK-neomycin* cassette, we intercrossed *Hand1*$^{Hand1+Neo}$ mice with the *EIIA-Cre* mouse line (Lakso et al., 1996), which expresses *Cre recombinase* systemically within the early mouse embryo. Mice carrying successfully recombined alleles (*Hand1*$^{Hand1\Delta Neo/+}$) were readily detected by RFLP shift via Southern blotting (Fig. 1A). Similar to *Hand1*$^{Hand1+Neo/Hand1+Neo}$ mice, we were unable to detect viable homozygous *Hand1*$^{Hand1\Delta Neo/Hand1\Delta Neo}$ offspring. Additionally, eGFP epiflorescence was not detectable at E9.5 (data not shown). Embryonic analyses indicate that *Hand1*$^{Hand1\Delta Neo/Hand1\Delta Neo}$ mice exhibited similar phenotypes to those of *Hand1*$^{Hand1+Neo/Hand1+Neo}$ embryos, but at a less severe penetrance (Fig 1B &C). Although the majority of embryos are viable to E10.5, 8% of the homozygous embryos are able to develop out to E12.5 where they display pericardial hemorrhaging, hypoplastic limb buds and craniofacial defects, as well as severe caudal defects, indicating that embryonic turning is compromised.

Hand1 expression analysis shows that *Hand1*$^{Hand1+Neo}$ and *Hand1*$^{Hand1\Delta Neo}$ alleles are hypomorphic

Given that the observed phenotypes associated with our *Hand1* cDNA knock-in alleles show some rescue of the *Hand1*$^{LacZ/LacZ}$ phenotype, we first looked at *Hand1* qualitative mRNA expression by whole mount and section *in situ* (Fig. 2). Whole mount analysis shows that *Hand1* mRNA is detectable in all viable wild type *Hand1*$^{Hand1+Neo/+}$ and *Hand1*$^{Hand1\Delta Neo/+}$ heterozygous mice and is indistinguishable in pattern and staining intensity. In contrast, homozygous *Hand1*$^{Hand1+Neo/Hand1+Neo}$ and *Hand1*$^{Hand1\Delta Neo/Hand1\Delta Neo}$ embryos appear to express lower, albeit still detectable, levels of *Hand1* mRNA (Fig. 2). Section *in situ* analysis reveals that the levels of *Hand1* expression are not uniformly reduced. For example, cardiac expression of *Hand1* is barely detectable, whereas pharyngeal arch expression appears more comparable to wild-type levels (Fig. 2F-H). *Hand2* mRNA expression is qualitatively similar and spatially independent of *Hand1* genotype (Fig. 3I-K). Given that we were unable to detect eGFP epiflorescence, we tested both *Hand1*$^{Hand1+Neo/Hand1+Neo}$ and *Hand1*$^{Hand1\Delta Neo/Hand1\Delta Neo}$ homozygous embryos for *eGFP* mRNA expression (Fig. L & M). Expression of *eGFP* mRNA is clearly detectable in a pattern identical to that of *Hand1* suggesting that the level of translated eGFP protein is simply below the threshold of our detection.

To gain an understanding of the overall decrease in expression of the *Hand1*$^{Hand1+Neo}$ and *Hand1*$^{Hand1\Delta Neo}$ alleles, we performed qRT-PCR using whole wild type, heterozygous, and homozygous *Hand1*$^{Hand1+Neo}$ and *Hand1*$^{Hand1\Delta Neo}$ E9.5 embryos, along with *Hand1*$^{LacZ/LacZ}$ null controls using *Taqman*-labeled primers that detect *Hand1*, *Hand2* and *Twist1* messages (Fig. 2N). Setting wild type *Hand1* levels as 100%, analysis of *Hand1*$^{Wt/LacZ}$ shows a significant ($P \leq 0.01$) 50% reduction in *Hand1* mRNA expression and, as expected, we were unable to detect *Hand1* expression in the *Hand1*$^{LacZ/LacZ}$ embryos. Expression analysis in *Hand1*$^{Hand1+Neo}$ heterozygous and homozygous mice shows higher levels of *Hand1* message than those of *Hand1* null mice. Heterozygous *Hand1*$^{Hand1+Neo}$

mice express approximately 90% of wild type expression levels, whereas *Hand1*$^{Hand1+Neo}$ homozygotes express *Hand1* at 50% that of wildtype, similar to the viable *Hand1*$^{+/LacZ}$ mice (P≤0.01) (Fig. 3N). *Hand1* expression in *Hand1*$^{+/Hand1\Delta Neo}$ heterozygotes is also 50% of wild-type; however, homozygotes express *Hand1* at only 30% of wild-type levels (P≤0.01). The lower level of *Hand1* mRNA expression observed, in conjunction with increased viability, suggests that there are possible translational differences that are *Pgk-neomycin* dependent and/or that expression within extraembryonic tissues (see Fig. 5) is more robust.

We next looked at *Hand2* expression in the various genotypes. It was previously reported that *Hand1* null mice show an upregulation of *Hand2* mRNA (Morikawa and Cserjesi, 2004). Consistent with this report, we see a reproducible 40% increase in *Hand2* expression within our *Hand1*$^{LacZ/LacZ}$ embryos as compared to wild-type controls; however, this increase is not statistically significant (P≥0.05). Interestingly, in contrast to *Hand1*$^{+/LacZ}$ embryos, which express wild type levels of *Hand2*, *Hand1*$^{Hand1+Neo}$ and *Hand1*$^{Hand1\Delta Neo}$ heterozygous and homozygous E9.5 embryos also exhibit a reproducible upregulation of *Hand2* mRNA, comparable to that observed in the *Hand1*$^{LacZ/LacZ}$ mice (Fig. 2L). Given that gene dosage phenotypes are reported for a number of Twist-family proteins and, specifically, *Hand1* and *Hand2* (McFadden et al., 2005), this alteration in gene balance is a possible mechanism that underlies the knock-in alleles' embryonic lethality despite that statistics suggest this increase in expression is not significant.

We also examined expression of *Twist1*, which codes for a potential dimer partner of Hand1 and shows genetic and functional interactions with Hand2 (Firulli et al., 2005). In *Hand1*$^{LacZ/LacZ}$ embryos, *Twist1* message is significantly reduced below 50% of what is observed in wild type littermates, whereas both *Hand1* homozygous hypomorphs express normal levels of *Twist1* mRNA (Fig. 2N). Given that *Hand1*$^{LacZ/LacZ}$ embryos are smaller and less viable, this observed decrease in *Twist1* expression could simply be a consequence of fewer mesenchymal cells within these embryos; however, collectively the changes observed in both *Hand2* and *Twist1* expression within the *Hand1*$^{LacZ/Lacz}$, *Hand1*$^{Hand1+Neo}$, and *Hand1*$^{Hand1\Delta Neo}$ homozygous alleles is a shared molecular characteristic between these engineered mouse models.

To further confirm that *Hand1*$^{Hand1+Neo}$ and *Hand1*$^{Hand1\Delta Neo}$ alleles were hypomorphic, we performed immunoblot analysis on E9.5 day embryos (Fig. 2O). HEK293 cells transfected with Hand1 were used to mark the size of Hand1 protein and to act as control for the Santa Cruz antisera. In wild-type and *Hand1* heterozygous null embryo lysates, the Hand1 antibody detects a protein that migrates similarly to what is observed in Hand1-transfected HEK293 lysates. This Hand1 band is not observed in equally loaded *Hand1*$^{LacZ/LacZ}$ embryo lysates suggesting that indeed this antibody is recognizing Hand1 protein. Similar to *Hand1* null embryos, *Hand1*$^{Hand1+Neo/Hand1+Neo}$ and *Hand1*$^{Hand1\Delta Neo/Hand1\Delta Neo}$ homozygous embryo lysates do not show detectable Hand1 protein expression. We conclude that there is a commensurate decrease in Hand1 translation such that levels of Hand1 protein are beyond the detection level of this antisera, but given that *Hand1*$^{Hand1+Neo/Hand1+Neo}$ and *Hand1*$^{Hand1\Delta Neo/Hand1\Delta Neo}$ embryos survive longer then *Hand1*$^{LacZ/LacZ}$ embryos a low level of Hand1 is indeed being translated and functionally active.

In order to gain a better understanding of these gross mutant phenotypes, a histological examination of *Hand1*$^{Hand1+Neo/Hand1+Neo}$ and *Hand1*$^{Hand1\Delta Neo/Hand1\Delta Neo}$ embryos was compared to wildtype littermates (Fig. 3). At E9.5, at the level of the cardiac OFT, *Hand1*$^{Hand1+Neo/Hand1+Neo}$ and *Hand1*$^{Hand1\Delta Neo/Hand1\Delta Neo}$ hearts are morphologically similar to what is observed in wild type littermates; however, key differences are observed. In *Hand1*$^{Hand1+Neo/Hand1+Neo}$ embryos, the heart is noticeably thinner (white arrowhead)

and dilated as compared to wild-type littermates. Pharyngeal mesoderm proximal to the OFT is reduced and a forming AP septum is not visible (Fig. 3A &B). At this stage, the mesenchymal cells, the majority of which are cardiac neural crest derived, are largely absent from the forming OFT cushions when compared to wild-type mice (Fig 3B asterisk). In contrast, *Hand1*$^{Hand1\Delta Neo/Hand1\Delta Neo}$ embryos appear phenotypically indistinguishable from wild type littermates at this age (Fig 3A, D &E, F). Comparison of the ventricular chamber at E9.5 reveals that *Hand1*$^{Hand1+Neo/Hand1+Neo}$ hearts are thin and hypotrabeculated; (Fig. D-E), whereas *Hand1*$^{Hand1\Delta Neo/Hand1\Delta Neo}$ hearts show a cardiac phenotype similar to wild-type littermates (Fig 3. D and F).

As a small percentage of *Hand1*$^{Hand1\Delta Neo/Hand1\Delta Neo}$ mice survive to E12.5, we examined hearts at this stage. Embryos show a slightly smaller size as compared to wild type and heterozygous littermates. Histology shows that *Hand1*$^{Hand1\Delta Neo/Hand1\Delta Neo}$ mice display reduced OFT cushions and decreased ventricular wall thickness in (Fig. 3G & H). At the level of the forming interventricular septum, septal cardiomyocytes are disorganized as compared to wild-type mice. Given that *Hand1*$^{LacZ/LacZ}$ embryos fail to undergo cardiac looping and embryonic turning (Firulli et al., 1998) there appears to be some level of phenotypic rescue from both cDNA expression alleles; however, given that the homozygote mice are non-viable, the overall expression from these hypomorphic *Hand1* alleles is insufficient.

We next compared the gene expression profiles for a number of putative Hand1 downstream targets expressed within the heart (Fig 3K). *Cited1,* which is expressed within the left ventricle, is down-regulated in *Hand1* conditional null mice (McFadden et al., 2005). Quantitative RT-PCR analysis from whole embryo RNA shows that in *Hand1*$^{LacZ/LacZ}$, *Hand1*$^{Hand1\Delta Neo/Hand1\Delta Neo}$, and *Hand1*$^{Hand1+Neo/Hand1+Neo}$ embryos, *Cited1* expression is also significantly ($P \leq 0.01$) reduced. *Chisel* expression, which is reported to be down-regulated in a *Hand1*-overexpression mouse model (Risebro et al., 2006) is also significantly down-regulated within all of our *Hand1* alleles (Fig 3L). Interestingly, *Atrial naturetic factor* (*Nppa*) which is downregulated in *Hand1* conditional null mice and is downregulated by more then 50% in systemic *Hand1* null and *Hand1*$^{Hand1+Neo/Hand1+Neo}$ embryos ($P \leq 0.01$) is only mildly downregulated within the *Hand1*$^{Hand1\Delta Neo/Hand1\Delta Neo}$ mice ($P \leq 0.05$) (Fig 3L). *Nkx2.5* lies directly upstream of *Hand1* and *Hand1* expression is downregulated in *Nkx2.5* null embryos (Lyons et al., 1995). *Nkx2.5* expression within *Hand1* null and *Hand1*$^{Hand1+Neo/Hand1+Neo}$ embryos shows a significant ($P \leq 0.01$) up-regulation suggesting a feed back regulatory mechanism. Although *Hand1*$^{Hand1\Delta Neo/Hand1\Delta Neo}$ embryos do exhibit a slight increase in *Nkx2*.5 expression, the levels are closer to what is observed in wild-type littermates and not significantly different ($P \geq 0.05$) (Fig 3L). Collectively, these histological and expression analyses suggest that the phenotypes observed with the null alleles are partially recapitulated within the *Hand1* cDNA alleles but that the less dramatic changes observed within the *Hand1*$^{Hand1\Delta Neo/Hand1\Delta Neo}$ homozygote embryos correlates with their extended lifespan.

Faulty mRNA processing is observed in *Hand1* hypomorphic alleles

To gain a better understanding as to why the *Hand1* cDNA knock-in alleles are hypomorphic, we employed RT-PCR to look specifically at *eGFP* and IVS *IRES* splicing. Defects in mRNA processing are a well-established cause of RNA degradation (Moore and Proudfoot, 2009). Primer sets that amplify only endogenously expressed *Hand1* confirm that *Hand1*$^{Hand1\Delta Neo/Hand1\Delta Neo}$ homozygous embryo genotypes are accurate (Fig. 4). As expected, *eGFP* mRNA is readily detectable in both heterozygous and homozygous *Hand1*$^{Hand1\Delta Neo}$ embryos but not in wild-type littermates. Interestingly, PCR across the IVS within the IRES cassette shows the presence of both unspliced and spliced *Hand1* chimeric

mRNA suggesting that the hypomorphic levels of expression result from faulty mRNA processing leading to message degradation and poor translation.

The primary *Hand1* hypomorphic phenotypes are extraembryonic and vascular insufficiency

Hand1 null mice display defects within the extraembryonic membranes that lead to nutrient insufficiencies that produce numerous secondary phenotypes leading to death (Firulli et al., 1998; Riley et al., 1998). *Pl1*, a growth factor essential for the maintenance of the corpus luteum, is significantly downregulated in *Hand1* null mice (Firulli et al., 1998; Riley et al., 1998). Therefore, we looked at *Pl1* expression in E9.5 placentas to assess *Pl1* expression in our hypomorphic *Hand1* alleles (Fig. 5). Transverse sections of wild-type embryo decidua show that *Hand1*-expressing trophoblast giant cells are co-expressing *Pl1* (Fig. 5A, B, F, G, K, and L). $Hand1^{Hand1+Neo}$ homozygous mice exhibit a marked reduction in *Pl1*-expressing cells (Fig. 5C, H, and M). $Hand1^{Hand1\Delta Neo}$ homozygous mice show reduced levels of *Pl1* expression as compared to wild-type mice, but visibly higher levels of expression then those observed in the $Hand1^{Hand1+Neo}$ homozygous embryos (Fig. 5D, I, N). As expected, $Hand1^{LacZ/LacZ}$ deciduas show the lowest level of *PL1* expressing cells (Fig. 5E, J, O). Given the importance of *Pl1* to embryonic survival, Hand1 regulation of *Pl1* is the likely contributor to embryonic death in both the systemic null and hypomorphic alleles.

To quantify the differences in *Pl1* gene expression, and to assay a number of other placental markers, we employed qRT-PCR analyses from E9.5 *Hand1* null and hypomorphic embryo placentas (Fig. 5P). As expected, the level of *Pl1* expression correlates directly with what is visibly observed by *in situ* analysis. The levels of *Pl1* message are significantly ($P \leq 0.01$) reduced by more then 50% in both hypomorphic alleles, which is significantly higher then the levels observed within the *Hand1* null placenta (Fig. 5P). Similar to the gene expression observations within the embryo, *Hand1* expression is not detectable within the *Hand1* null placenta where as $Hand1^{Hand1+Neo}$ homozygous express very low but detectable levels of *Hand1* expression. Additionally, the $Hand1^{Hand1\Delta Neo/Hand1\Delta Neo}$ placenta expresses *Hand1* at approximately 30% of the wild type placenta levels of *Hand1* (Fig 5P). This result may clarify why $Hand1^{Hand1\Delta Neo/Hand1\Delta Neo}$ embryos survive longer then $Hand1^{Hand1+Neo}$ homozygous embryos even though the $Hand1^{Hand1\Delta Neo/Hand1\Delta Neo}$ embryos exhibit lower levels of embryonic *Hand1* expression (Fig 2N). Consistent with the embryonic analysis, the message for *Hand2* within the placenta is observed to be upregulated; however, in contrast, *Twist1* mRNA levels are not down-regulated and are observed to be at the same level or at a slightly higher level of expression than is observed within the wild-type placenta (Fig. 2N & 5P). *Cited1*, in addition to being expressed within the heart, is also expressed within the placenta. Consistent with the cardiac expression data, *Cited1* expression is markedly down in both the null and hypomorphic *Hand1* placentas ($P \leq 0.01$) (Fig 5P). *Membrane metallo endopeptidase (Mme; also known as 4311*) is shown to exhibit expanded expression in *Hand1* null conceptus (Riley et al., 1998). Consistent with these findings, we observe an increase in *Mme* expression within the *Hand1* null and hypomorphic placenta but this increase is only significant in $Hand1^{Hand1\Delta Neo/Hand1\Delta Neo}$ placenta (Fig. 5P). Expression of *matrix metallopeptidase 9* (*Mmp9*) is also upregulated in both *Hand1* null and *Hand1* hypomorphic alleles. *LimK* and *Mash2* are reported as being down-regulated and up-regulated in *Hand1* null mice respectively (Riley et al., 1998). We observe near normal levels of *Limk* in *Hand1* null and hypomorphic mice (Fig. 5P). The expression levels of *Mash2* appear indistinguishable from the wild-type placenta expression levels.

In addition to trophoblast giant cell gene expression, defects within the yolk sac vascular development, and associated changes in gene expression, are observed in *Hand1* null embryos (Morikawa and Cserjesi, 2004). To determine if our *Hand1* hypomorphic alleles display similar or distinct vascular expression profiles as compared to the *Hand1* null mice,

we performed quantitative RT-PCR to compare expression (Fig 5Q). Expression of the angiogenic growth factor *Angpt1* is up-regulated within *Hand1* null mice. We observe a significant (P≤0.01) 2-fold up-regulation of *Angpt1* in *Hand1* null embryos consistent to published reports (Fig. 5Q; (Morikawa and Cserjesi, 2004)). Both hypomorphic *Hand1* alleles show comparable increases in *Angpt1* expression. Upregulation of *Vegf* and *Flt1* within in hypomorphic *Hand1* mice is indistinguishable from systemic null *Hand1* analysis. In contrast, we observe a decrease in the expression of *Flk1* within systemic and $Hand1^{Hand1\Delta Neo}$ homozygous embryos; however, expression in $Hand1^{Hand1+Neo}$ homozygous embryos is slightly elevated in a consistent but not statistically significant frequency (Fig. 5Q). Thymosin β4 is an important contributor to the coronary vasculature and was identified has a Hand1 downstream target (Smart et al., 2002). Analysis of *Thymosin β4* expression in *Hand1* systemic null mice validates these findings showing a significant (P≤0.01) 50% decrease in expression (Fig. 5Q). Similarly, both hypomorphic *Hand1* alleles show near identical decreases in *Thymosin β4* expression. Given its role in inducing angiogenesis and as hypoxia sensor, we looked at expression of the PAS-family bHLH transcription factor Hif-1α. Hif-1α is known to induce Vegf. Surprisingly, we observed a significant (P≤0.05) 50% reduction in *Hif-1α* mRNA in *Hand1* systemic null and *Hand1* hypomorphic embryos (Fig. 5Q). Given that Hif-1α should promote vessel formation, we were initially surprised to see a reduction in expression; however, *Hif-1α* knockout mice display abnormal vascular development and embryonic lethality, which is also associated with an upregulation of *Vegf*. (Ryan et al., 1998; Kotch et al., 1999). Taken together, the consistent similarity in changes observed in vascular gene expression between the *Hand1* null and hypomorphic mice suggests that these defects, in combination with giant cell abnormalities, ultimately result in embryonic death. Extension of hypomorphic embryo survival is attributable to a substantial improvement in cardiac morphology and diminished alterations in cardiac gene expression.

To better define the extent of placental and vascular insufficiencies in the *Hand1* hypomorphic phenotype, we performed cell death and cell proliferation analysis at E9.5 and E11.5 in wild-type, $Hand1^{Hand1+Neo}$ (E9.5), and $Hand1^{Hand1\Delta Neo}$ (E 9.5 and E11.5) homozygous mice (Fig. 6). Apoptosis levels were indistinguishable between wild-type and *Hand1* hypomorphic mice at E9.5 and E11.5. In contrast, BrdU incorporation analysis performed at E9.5 reveals a global decrease in the rate of cell proliferation in $Hand1^{Hand1+Neo/Hand1+Neo}$ $Hand1^{Hand1\Delta Neo/Hand1\Delta Neo}$ embryos compared to wildtype controls, indicating that the placental and vascular defects observed are globally affecting embryo viability. Taken together, these data correlate the severity of the observed *Hand1* allelic phenotypes with the placental viability and support the hypothesis that the extraembryonic sources lead to the primary phenotypes that result in embryonic death where insufficiencies first slow and then stall embryogenesis.

Loss of *Hand2* enhances *Hand1* hypomorphic defects

One of the key observations made in Morikawa *et. al*. and that we confirm is the up-regulation of the highly related transcription factor *Hand2*. There is a robust and growing body of data showing that members of the Twist-family of bHLH proteins have a functional sensitivity to gene dosage. In fact, Twist-family mutant phenotypes become more severe or exhibit phenotypic rescue when haploinsufficiency of other family members is introduced onto the mutant background (Firulli et al., 2005; McFadden et al., 2005). Thus, we crossed $Hand1^{Hand1\Delta Neo}$ heterozygous mice onto the *Hand2* systemic null background to deduce if a reduction in the upregulation of *Hand2* would result in more severe embryonic phenotypes or further rescue the hypomorphic allele.

Our results show that $Hand1^{Hand1\Delta Neo/Hand1\Delta Neo}$ embryos that are also heterozygous for *Hand2* are phenotypically indistinguishable from mice wild type for *Hand2* (data not

shown). Given the lack of phenotypic change of the hypomorphic mice on a *Hand2* heterozygous null background, we next looked at $Hand1^{Hand1\Delta Neo/Hand1\Delta Neo}$ embryos on a *Hand2* homozygous null (Fig. 7). *Hand2* null, *Hand1* hypomorph embryos are significantly smaller and display poor caudal development as compared to *Hand2* null and *Hand1* hypomorphic mice alone (Fig. 7A-D). Cardiac morphology shows that cardiac morphogenesis is comparable to both *Hand1* hypomorph and *Hand2* null littermates with regards to looping; however, sections through the myocardium show a thin ventricular wall. As discussed above, $Hand1^{Hand1\Delta Neo/Hand1\Delta Neo}$ hearts at E9.5–10.5 are similar in morphology to wild type (Fig. 7E and F). Consistent with published findings, *Hand2* null embryos show a thin myocardium and a reduced/absent right ventricle (Fig. 7F) (Srivastava et al., 1997). Although it is possible that these data suggest genetic interactions within the developing heart, given that Hand factors are co-expressed within lateral mesoderm and, specifically, the vessels that connect to the placenta, these cardiac defects could be secondary to the placental insufficiencies.

DISCUSSION

In our efforts to generate a *Hand1* marked allele, we inadvertently generated two *Hand1* hypomorphic mouse models, which partially extend the viability of *Hand1* loss-of-function. The phenotypic cause of death is the result of both placental and vascular insufficiency and is further supported by our observations of decreased numbers of *PL1*-expressing trophoblast giant cells and changes within the vascular gene expression profile. Collectively, these defects result in a global reduction of cell proliferation within homozygous hypomorphic *Hand1* mice. In *Hand1* over-expressing mice, there is an observed increase of proliferation within the cardiomyocytes (Risebro et al., 2006). In both of our hypomorphic *Hand1* alleles, we observe a global decrease in cell proliferation (Fig 6). Clearly, much of this reduction is a result of placental and vascular insufficiency; however, it is possible that additional decreases in proliferation within the cardiomyocytes and neural crest have a cell autonomous contribution to the phenotype.

In principle, designing targeting constructs to express a fully processed cDNA is a straightforward approach; however, in practice, unforeseen difficulties may be encountered. We show that using an IRES to allow bicistronic coexpression of both a reporter allele (*eGFP*) and *Hand1*, which appears functional in tissue culture applications, does not function well in mice (Fig 4). Although the *Hand1* and *eGFP* mRNA is expressed, the protein expression of either Hand1 or eGFP is beyond detection with available reagents. Our only evidence that there is *bona-fide* translation of the Hand1 protein is the extended survival of both hypomorphic alleles when compared to what is observed in *Hand1* systemic deletion. It is possible that the differences in targeting construct design could account for these observations, but we feel that this is unlikely as we employed identical 5′ and 3′ targeting arms to those that were used to generate our null allele (Fig. 1) (Firulli et al., 1998). Given that we do observe *Hand1* mRNA, whereas in the *Hand1* null mice we do not (Fig. 2), this is the likely mechanism for increased phenotypic viability. To achieve our intended goal of generating a *Hand1* marker allele that does not effect bHLH gene dosage will possibly require knocking the reporter cassette into the intron or directly targeting the reporter into a bacterial artificial chromosome clone containing all transcriptional modules necessary to recapitulate endogenous expression.

The extension of viability observed in homozygous *Hand1* hypomorphic embryos to between E10.5–12.5 reveals that cardiac morphogenesis is largely normal. Phenotypic distinctions include thin myocardium, hypo-trabeculation, and a reduction in pharyngeal mesoderm and OFT mesenchyme which are likely direct effects given the expression of *Hand1* in these tissues. These phenotypes, if isolated, would likely allow for survival until

birth. Cardiac specific deletion of *Hand1* results in perinatal death (McFadden et al., 2005). As our hypomorphic alleles include similar placental and vascular defects to *Hand1* systemic null embryos, we can deduce that the improvement in cardiac morphology contributes directly to the increased survival and maybe the result of the low level of Hand1 protein present within these tissues. Indeed, we observe differences between the three mutant *Hand1* alleles in a set of cardiac expressed factors. *Nppa*, for example, is clearly downregulated in the *Hand1* null; however, expression in $Hand1^{Hand1\Delta Neo/Hand1\Delta Neo}$ clearly shows more robust expression correlating with this alleles improved survival (Fig. 3).

The quantitative measure of *Hand1* expression from both the $Hand1^{Hand1+Neo}$ and $Hand1^{Hand1\Delta Neo}$ hypomorphic alleles defines the range of required *Hand1* expression as between 15% and 20% from each allele of that observed from the wild type alleles. *Hand1* heterozygous null mice are viable and display no obvious phenotypes. *Hand1* homozygous null mice die at E8.5 and show no detectable *Hand1* mRNA, confirming that $Hand1^{LacZ}$ is a true null allele. As hypomorphic *Hand1* embryos are larger, further developed, and express 30–40% of the wild-type level of *Hand1*, it is clear that a precise gene dosage of *Hand1* is critical and that expression slightly less then haploinsufficiency is deleterious to survival. Comparison of the *Hand1* expression levels between heterozygous $Hand1^{+/LacZ}$ and $Hand1^{Hand1+Neo/Hand1+Neo}$ and $Hand1^{Hand1\Delta Neo/Hand1\Delta Neo}$ E9.5 day embryos show no significant differences, yet the former genotype is viable whereas the latter genotypes are not. It is possible that the engineered cDNA alleles lack key processing sequences that allow for efficient translation of Hand1 protein. Indeed, we have determined that allele splicing is inefficient and the lack of the complete 3′ untranslated region within these *Hand1* alleles may directly point to post-transcriptional regulation such as micro RNAs that refine *Hand1* expression to meet the developmental program requirements of the cell. Additionally, the improperly processed mRNA can also contribute to less-efficient translation as evidenced by the inability to detect Hand1 protein in homozygous hypomorphs where protein is detectable in wild-type and heterozygous null littermates (Fig. 2). Perhaps most interesting is the observed up-regulation of *Hand2* within the null and hypomorphic mice. Early studies on *Hand1* and *Hand2* suggested functional redundancy (Srivastava et al., 1995). In such a biological relationship, the up-regulation of *Hand2* to compensate for the loss of *Hand1* is logical. Additionally, strong genetic interactions between Twist-family proteins are observed between *Hand2* with *Twist1* within the developing limb (Firulli et al., 2005). To test if the observed up-regulation of *Hand2* is indeed a compensatory mechanism or a deleterious dysregulation, we looked at hypomorphic $Hand1^{Hand1\Delta Neo/Hand1\Delta Neo}$ mice on both a *Hand2* heterozygous and homozygous null background. *Hand2* heterozygousity showed no significant change to the observed *Hand1*-hypomorphic phenotypes suggesting genetic interactions are not significantly affected in this genotype. Evaluation of *Hand1* hypomorphs devoid of *Hand2* expression do show observable differences in that embryos are smaller and display reduced caudle structures and thin lateral mesoderm similar to *Hand1* hypomorphs (Fig. 2 and 7). Cardiogenesis occurs but the wall of the heart is extremely thin. This result could be direct via *bona fide* genetic interactions within the myocardium; however, it is more likely that additive effects or genetic effects within the placenta connections exacerbate the *Hand1* hypomorphic extraembryonic phenotypes.

The role of Twist-family bHLH factors in embryonic development is complex. Given that these factors function biologically within a variety of dimer complexes makes evaluation of their role in gene expression and cell specification and differentiation difficult. Dimer partner choice can result in the formation of multiple transcriptional complexes that may regulate different genes sets or the same gene sets in different ways. An example of this can be seen with Twist in *drosophila* where it has been shown that Twist homodimers promote somatic muscle formation, whereas Twist-daughterless (E-protein) heterodimers antagonize somatic muscle formation (Castanon et al., 2001). Considering the removal of a single

bHLH gene from a cell, it is obvious that the interactive relationships of the remaining factors within that cell must change. The formation of inappropriate dimers is a likely outcome and whether these dimers are benign or functionally deleterious is likely going to be dictated by a cell type specific relationship. In summary, in our efforts to produce a *Hand1* expression reporter that does not affect *Hand1* gene dosage, we generated two alleles that express low levels of *Hand1*. Where in systemic and conditional *Hand1* alleles 100% ablation is achieved, the $Hand1^{Hand1+Neo}$ and $Hand1^{Hand1\Delta Neo}$ hypomorphic mice demonstrate that normal development cannot tolerate less then 30% of *Hand1* within the embryo or extra-embryonic structures.

EXPERIMENTAL PROCEDURES

Plasmid Constructs

The *Hand* $^{Hand1+neo}$ targeting vector employed the identical 5′ and 3′ targeting arms employed in generation of the $Hand1^{Laz}$ knock-in (Firulli et al., 1998). Inserted between these arms is a *Hand1* cDNA that begins 70 base pairs 5′ of the initiating methionine and ends at the translational stop site. The *Hand1* cDNA is immediately 5′ of an IRESGFP cassette derived from pIRESeGFP (Clonetech), which is immediately 5′ of a PGKNeo cassette flanked by loxP sites. Homologous recombination was achieved at a frequency of one in fifteen and two independent ES lines were injected and produced germline transmission with indistinguishable phenotypes.

Mouse strains

$Hand1^{Hand1+neo}$ mice were generated by the IU knockout-transgenic core from ES cells targeted with the construct described above. $Hand^{Hand1\Delta neo}$ mice were subsequently generated via intercross of *Hand* $^{Hand1+neo}$ mice with mice heterozygous for *EIIA-Cre* allele (Lakso et al., 1996). Both versions of the reporter allele are viable and fertile as heterozygotes. $Hand1^{Laz}$ knock-in mice have been reported previously (Firulli et al., 1998) and *Hand2* knockout (Srivastava et al., 1997) mice have been reported previously.

Histology

Embryos (E9.5 – E11.5) were fixed in 4% paraformaldehyde, dehydrated through an ethanol gradient and embedded in paraffin. Embryos were sectioned at 7μm unless otherwise noted. Hematoxylin and Eosin (H&E) staining was performed exactly as described (Conway et al., 2000). A minimum of 3 viable embryos (assayed via the presence of a heart beat) per genotype was used for these and all subsequent analyses.

In situ hybridization-qRT-PCR

Digoxygenin labeled section *in situ* hybridizations were carried out using established protocols on 10μm paraffin sections or in whole mount (Vincentz et al., 2008) using T7, T3 or SP6 polymerases (Promega) and DIG-Labeling Mix (Roche). Sense and antisense digoxygenin-labeled riboprobes were transcribed for *Hand1*, *Hand2*, *eGFP*, and *Pl1*. Hybridizations and all subsequent incubations were done concurrently on all embryos being compared. qRT-PCR was performed on a Lightcycler 480II (Roche) using Taqman labeled proprietary primer sets for *Hand1*, *Hand2* and *Gapdh* as internal control. Gene expression for marker genes was performed using Taqman primers or via the Roche UPL (universal probe library, mouse) system. Whole embryos, placentas, or yolk sacs were flash frozen and genotyped via genomic DNA from the yolk sac or head of the embryo. Total RNA was isolated using a High Pure RNA Tissue kit (Roche) and cDNA was prepared using the Transcriptor First Strand cDNA synthesis kit (Roche) following the manufactures protocol. A minimum of 4 viable embryos (assayed via the presence of a heart beat) were analyzed in

all experiments. Error bars denote standard error. Differences between mouse lines were examined for statistical significance by using the Students t-test. P values of less than 0.05 were regarded as significant and marked in all graphs as a single asterisk * and P values less then 0.01 are denoted with double asterisk **

Immunoblotting

Embryo lysates were collected, and equal amounts of protein were run through 12% SDS PAGE gels, electroblotted and incubated with α-Hand1 polyclonal antibody (Santa Cruz) as described (Firulli et al., 2003). Blots were visualized using the Super Signal Luminescent detection protocol (Pierce).

TUNEL and Immunohistochemistry

TUNEL analysis on sectioned embryos was performed using the *ApopTag Plus* Fluorescein *in situ* Apoptosis detection kit (S7111 Chemicon International) following the manufacturers instructions. Cell proliferation was assayed using Bromodeoxy Uridine (BrdU) incorporation and immunodetection following the manufacturer's instructions. For embryos, time-mated females were injected IP with BrdU (100ug/g body weight) 2 hours prior to sacrifice. Embryos were processed as described above and then cut transverse in 7μm sections. Immunohistochemistry was performed using α-BrdU (Abcam), developed using a standard streptavidin-HRP method, and counterstained with Hematoxylin.

Acknowledgments

We would like to thank Danny Carney and Santiago Pineda for technical assistance. Infrastructural support at the Herman B Wells Center for Pediatric Research is in part supported by the generosity of the Riley Children's Foundation and Division of Pediatric Cardiology. This work is supported by the NIH RO1HL061677-09 1P01HL085098-01A (ABF), and AHA 0815426G (RMB).

Grant Sponsor: NIH RO1HL061677-09 1P01HL085098-01A (ABF), and AHA 0815426G (RMB).

References

Barnes RM, Firulli AB. A Twist of insight, the role of Twist-Family bHLH factors in development. Int J Dev Biol. 2009; 53:909–924. [PubMed: 19378251]

Castanon I, Von Stetina S, Kass J, Baylies MK. Dimerization partners determine the activity of the Twist bHLH protein during Drosophila mesoderm development. Development. 2001; 128:3145–3159. [PubMed: 11688563]

Conway SJ, Bundy J, Chen J, Dickman E, Rogers R, Will BM. Decreased neural crest stem cell expansion is responsible for the conotruncal heart defects within the splotch (Sp(2H))/Pax3 mouse mutant.[see comment]. Cardiovascular Research. 2000; 47:314–328. [PubMed: 10946068]

Firulli AB. A HANDful of questions: The molecular biology of the HAND-subclass of basic helix-loop-helix transcription factors. Gene. 2003; 312C:27–40. [PubMed: 12909338]

Firulli AB, Conway SJ. Phosphoregulation of Twist1 provides a mechanism of cell fate control. Current Medicinal Chemistry. 2008; 15:2641–2647. [PubMed: 18855684]

Firulli AB, McFadden DG, Lin Q, Srivastava D, Olson EN. Heart and extra-embryonic mesodermal defects in mouse embryos lacking the bHLH transcription factor Hand1. Nature Genetics. 1998; 18:266–270. [PubMed: 9500550]

Firulli B, Howard MJ, McDaid JR, McIlreavey L, Dionne KM, Centonze V, Cserjesi P, Virshup DMa, Firulli AB. PKA, PKC and the Protein Phosphatase 2A Influence HAND factor function: A Mechanisms for Tissue Specific Transcriptional Regulation. Mol Cell. 2003; 12:1225–1237. [PubMed: 14636580]

Firulli BA, Krawchuk D, Centonze VE, Virshup DE, Conway SJ, Cserjesi P, Laufer E, Firulli AB. Altered Twist1 and Hand2 dimerization is associated with Saethre-Chotzen syndrome and limb abnormalities. Nat Genet. 2005; 37:373–381. [PubMed: 15735646]

Kotch LE, Iyer NV, Laughner E, Semenza GL. Defective vascularization of HIF-1α-null embryos is not associated with VEGF deficiency but with mesenchymal cell death. Dev Biol. 1999; 209:254–267. [PubMed: 10328919]

Lakso M, Pichel JG, Gorman JR, Sauer B, Okamoto Y, Lee E, Alts FW, Westphal H. Efficient in vivo manipulation of mouse genomic sequences at the zygote stage. Proc Natl Acad Sci USA. 1996; 93:5860–5865. [PubMed: 8650183]

Lyons I, Parsons LM, Hartley L, Li R, Andrews JE, Robb L, Harvey RP. Myogenic and morphogenetic defects in the heart tubes of murine embryos lacking the homeo box gene Nkx2–5. Genes Dev. 1995; 9:1654–1666. [PubMed: 7628699]

McFadden DG, Barbosa AC, Richardson JA, Schneider MD, Srivastava D, Olson EN. The Hand1 and Hand2 transcription factors regulate expansion of the embryonic cardiac ventricles in a gene dosage-dependent manner. Development. 2005; 132:189–201. [PubMed: 15576406]

Moore MJ, Proudfoot NJ. Pre-mRNA processing reaches back to transcription and ahead to translation. Cell. 2009; 136:688–700. [PubMed: 19239889]

Morikawa Y, Cserjesi P. Extra-embryonic vasculature development is regulated by the transcription factor HAND1. Development. 2004; 131:2195–2204. [PubMed: 15073150]

Riley P, Anson-Cartwright L, Cross JC. The Hand1 bHLH transcription factor is essential for placentation and cardiac morphogenesis. Nat Genet. 1998; 18:271–275. [PubMed: 9500551]

Risebro CA, Smart N, Dupays L, Breckenridge R, Mohun TJ, Riley PR. Hand1 regulates cardiomyocyte proliferation versus differentiation in the developing heart. Development. 2006; 133:4595–4606. [PubMed: 17050624]

Ryan HE, Lo J, Johnson RS. HIF-1α is required for solid tumor formation and embryonic vascularization. EMBO J. 1998; 17:3005–3015. [PubMed: 9606183]

Smart N, Hill AA, Cross JC, Riley PR. A differential screen for putative targets of the bHLH transcription factor Hand1 in cardiac morphogenesis. Gene Expression Patterns. 2002; 2:61–67. [PubMed: 12617838]

Srivastava D, Cserjesi P, Olson EN. A subclass of bHLH proteins required for cardiac morphogenesis. Science. 1995; 270:1995–1999. [PubMed: 8533092]

Srivastava D, Thomas T, Lin Q, Kirby ML, Brown D, Olson EN. Regulation of cardiac mesodermal and neural crest development by the bHLH transcription factor, dHAND. Nature Genetics. 1997; 16:154–160. [PubMed: 9171826]

Vincentz JW, BArnes RM, Rodgers R, Firulli BA, Conway SJ, Firulli AB. An Absence of Twist1 results in aberrant cardiac neural crest morphogenesis. Dev Biol. 2008; 320:131–139. [PubMed: 18539270]

Walker WH, Fitzpatrick SL, Barrera-Saldana HA, Resendez-Perez D, Saunders GF. The human placental lactogen genes: structure, function, evolution and transcriptional regulation. Endocrine Reviews. 1991; 12:316–328. [PubMed: 1760991]

Yamaguchi M, Ogren L, Endo H, Soares MJ, Talamantes F. Co-localization of placental lactogen-I, placental lactogen-II, and proliferin in the mouse placenta at midpregnancy. Biology of Reproduction. 1994; 51:1188–1192. [PubMed: 7888496]

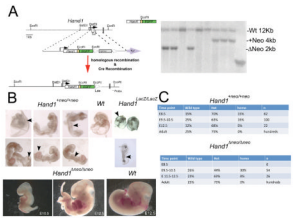

Figure 1.

(A) Schematic of Hand1cDNA targeting vector and southern blot showing RFLP identification of the +Neo and ΔNeo alleles. (B) Wholemount view of $Hand1^{Hand1+Neo/Hand1+Neo}$, $Hand1^{Lacz/LacZ}$ and wild type E9.5 day embryos. $Hand1^{Hand1+Neo/Hand1+Neo}$ embryos display thickened “blistered” yolk sac (arrow left panels) enlarged allantois (arrowhead) and crooked neural tube indicative of placental insufficiency. These phenotypes are observed and more severe in $Hand1^{Lacz/LacZ}$ embryos (right panels). $Hand1^{Hand1+Neo/Hand1+Neo}$ embryos display a generally normal looking looped heart as compared to $Hand1^{Lacz/LacZ}$ mice. E10.5 and E12.5 $Hand1^{Hand1\Delta Neo/Hand1\Delta Neo}$ embryos display caudal defects in lateral mesoderm and hypoplastic limb buds as compared to wild type littermates. Hearts of $Hand1^{Hand1\Delta Neo/Hand1\Delta Neo}$ embryos are looped and morphologically similar to wildtype. (C) Genotypic analysis at E8.5–E12.5 & adult stages for occurrence of $Hand1^{Hand1+Neo/Hand1+Neo}$ and $Hand1^{Hand1\Delta Neo/Hand1\Delta Neo}$ mice. $Hand1^{Hand1+Neo/Hand1+Neo}$ embryos are detectable at slightly lower then expected mendellian ratios up to E10.5 and are completely lost by E12.5. $Hand1^{Hand1\Delta Neo/Hand1\Delta Neo}$ embryos are detectable at expected frequencies until E12.5 where they are observed at 8% frequency. $Hand1^{Lacz/LacZ}$ mice are not detected beyond E9.5 (Firulli et al., 1998; Riley et al., 1998, Morikawa, 2004 #2340).

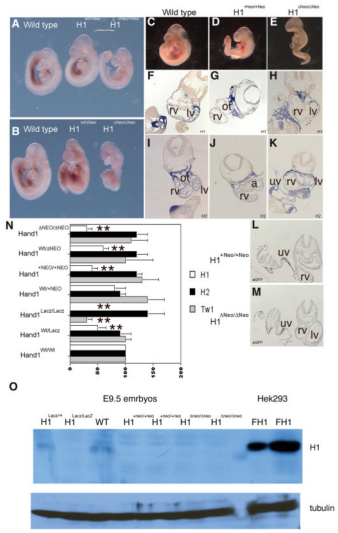

Figure 2.

(A and B) Whole mount *Hand1 in situ* hybridization in wildtype, heterozygous and homozygous $Hand1^{Hand1+Neo/Hand1+Neo}$ *and* $Hand1^{Hand1\Delta Neo/Hand1\Delta Neo}$ E9.5 embryos. Expression is observed in pharyngeal arches, lateral mesoderm, and left ventricle in all genotypes; however mRNA is reduced in both $Hand1^{Hand1+Neo/Hand1+Neo}$ *and* $Hand1^{Hand1\Delta Neo/Hand1\Delta Neo}$ homozygous mice. Section *in situ* for *Hand1* (F, G, H), *Hand2* (I, J, K), and *eGFP* (L and M). *Hand1* expression appears reduced within the myocardium of the left ventricle whereas expression through pharyngeal and lateral mesoderm appears closer to wild type levels in both $Hand1^{Hand1+Neo/Hand1+Neo}$ *and* $Hand1^{Hand1\Delta Neo/Hand1\Delta Neo}$ homozygous mice. *Hand2* expression is spatially unaffected in within the *Hand1* cDNA homozygous mice showing expected expression within the neural crest of the outflow track, heart, pharyngeal and lateral mesoderm. Analysis of eGFP expression shows that in both $Hand1^{Hand1+Neo/Hand1+Neo}$ *and* $Hand1^{Hand1\Delta Neo/Hand1\Delta Neo}$ homozygous mice eGFP message is detectable and expressed in an identical spatial pattern to what is observed for *Hand1*. rv, right ventricle; lv, left ventricle; ot, outflow tract; uv umbilical vein. (N) Quantitative RT PCR using Taqman primers specific for Hand1, Hand2 and Twist1 message. In $Hand1^{Lacz/LacZ}$ heterozygous and homozygous null mice, a 50% and 100% reduction in Hand1 message is observed. $Hand1^{Hand1+Neo/Hand1+Neo}$ heterozygous mice express Hand1 at wild type levels whereas homozygous mice express Hand1 at 40% of that observed in wildtype. $Hand1^{Hand1\Delta Neo/Hand1\Delta Neo}$ heterozygous mice express *Hand1* at 50% and homozygous 30% of that observed in wildtype. Hand2 expression is upregulated in $Hand1^{Lacz/LacZ}$ embryos as well as in $Hand1^{Hand1+Neo/Hand1+Neo}$ *and* $Hand1^{Hand1\Delta Neo/Hand1\Delta Neo}$ homozygous embryos. Twist1 expression is reduced to 40% of wildtype levels in $Hand1^{Lacz/LacZ}$ null mice; however, Twist1 expression is within the wildtype range in both $Hand1^{Hand1+Neo/Hand1+Neo}$ *and* $Hand1^{Hand1\Delta Neo/Hand1\Delta Neo}$ homozygous embryos. (O). Immunoblot detection of Hand1 protein in E9.5 embryos and HEK293cells transfected with pcDNA flagHand1. Protein is observed in wildtype embryos; however, the level of protein is beyond the sensitivity of the antibody in $Hand1^{Hand1+Neo/Hand1+Neo}$ *and* $Hand1^{Hand1\Delta Neo/Hand1\Delta Neo}$ homozygous embryos. Error bars denote standard error, * indicates a P value of less than or equal to 0.05 and ** indicates a P value of less than or equal to 0.01.

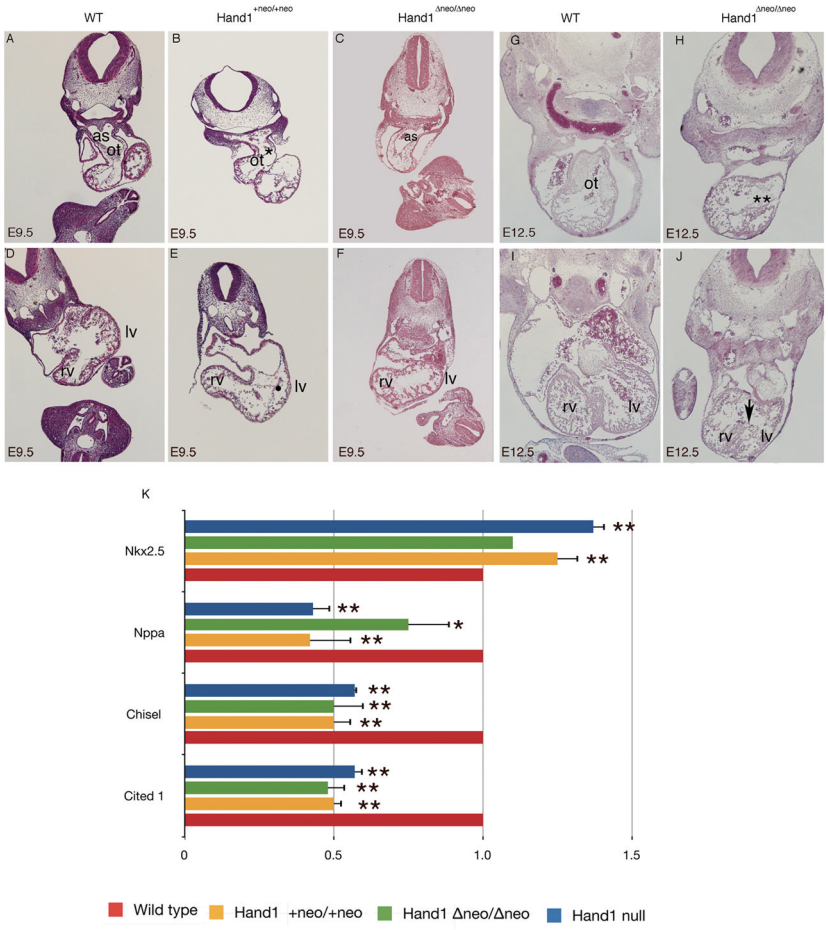

Figure 3.

H&E histological analysis of E9.5 day *Hand1*$^{Hand1+Neo/Hand1+Neo}$ (B, E) and *Hand1*$^{Hand1\Delta Neo/Hand1\Delta Neo}$ (C, F). Compared to wild type littermates (A,D) *Hand1*$^{Hand1+Neo/Hand1+Neo}$ embryos display thin hypotrabeculated hearts (white arrowhead) and a reduced number of mesenchymal cells within the outflow track (ot) (*). Pharyngeal mesenchyme is also reduced and lacks a forming aortic septum (as). In contrast at E9.5 *Hand1*$^{Hand1\Delta Neo/Hand1\Delta Neo}$ embryo hearts appear phenotypically normal. Histological analysis of E12.5 *Hand1*$^{Hand1\Delta Neo/Hand1\Delta Neo}$ embryos (H, J) reveals a largely acellular outflow track cushion (**) and poorly organized interventricular septum (white arrow) when compared to a wild type littermate (G, I). rv, right ventricle; lv, left ventricle. Quantitative RTPCR analysis from E9.5 day Hand1 systemic null, *Hand1*$^{Hand1+Neo/Hand1+Neo}$ and *Hand1*$^{Hand1\Delta Neo/Hand1\Delta Neo}$ embryos (K). Data represents the mean of at least 4 embryos and error bars denote standard error, * indicates a P value of less than or equal to 0.05 and ** indicates a P value of less than or equal to 0.01

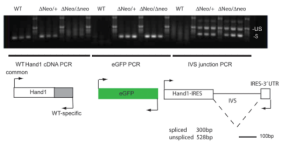

Figure 4.

RTPCR analysis of expressed *Hand1* message from *Hand1*$^{Hand1\Delta Neo}$ heterozygous and homozygous embryos. PCR primers designed to detect endogenous, eGFP and IRES-IVS splice junctions were employed to amplify cDNA pools generated from whole embryos of the indicated genotypes. IVS primers detect both spliced and un-spliced *Hand1IreseGFP* message.

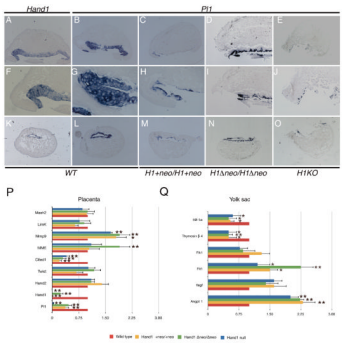

Figure 5.

Expression of PL1 in placentas from wildtype, *Hand1*$^{Lacz/LacZ}$, *Hand1*$^{Hand1+Neo/Hand1+Neo}$ *and Hand1*$^{Hand1\Delta Neo/Hand1\Delta Neo}$ homozygous E9.5 embryos. (A,F,K) Expression of *Hand1* in wild-type decidua. (B, G, L) Expression of *PL1* in wild-type littermates. (C, H, M) *PL1* expression in *Hand1*$^{Hand1+Neo/Hand1+Neo}$ embryos shows a reduced level of PL1 positive cells. (D, I, N) *PL1* expression in *Hand1*$^{Hand1\Delta Neo/Hand1\Delta Neo}$ embryos is observed to be less the wild type but higher then in *Hand1*$^{Hand1+Neo/Hand1+Neo}$ embryos. (E, J, O). *PL1* expression studies in *Hand1*$^{Lacz/LacZ}$ embryos show nearly a complete loss of *PL1*-expressing cells. (P) Comparative qRT-PCR analysis of vascular markers in wildtype, null and hypomorphic Hand1 embryos. A minimum of 4 embryos for each genotype were employed and error bars denote standard error, * indicates a P value of less than or equal to 0.05 and ** indicates a P value of less than or equal to 0.01

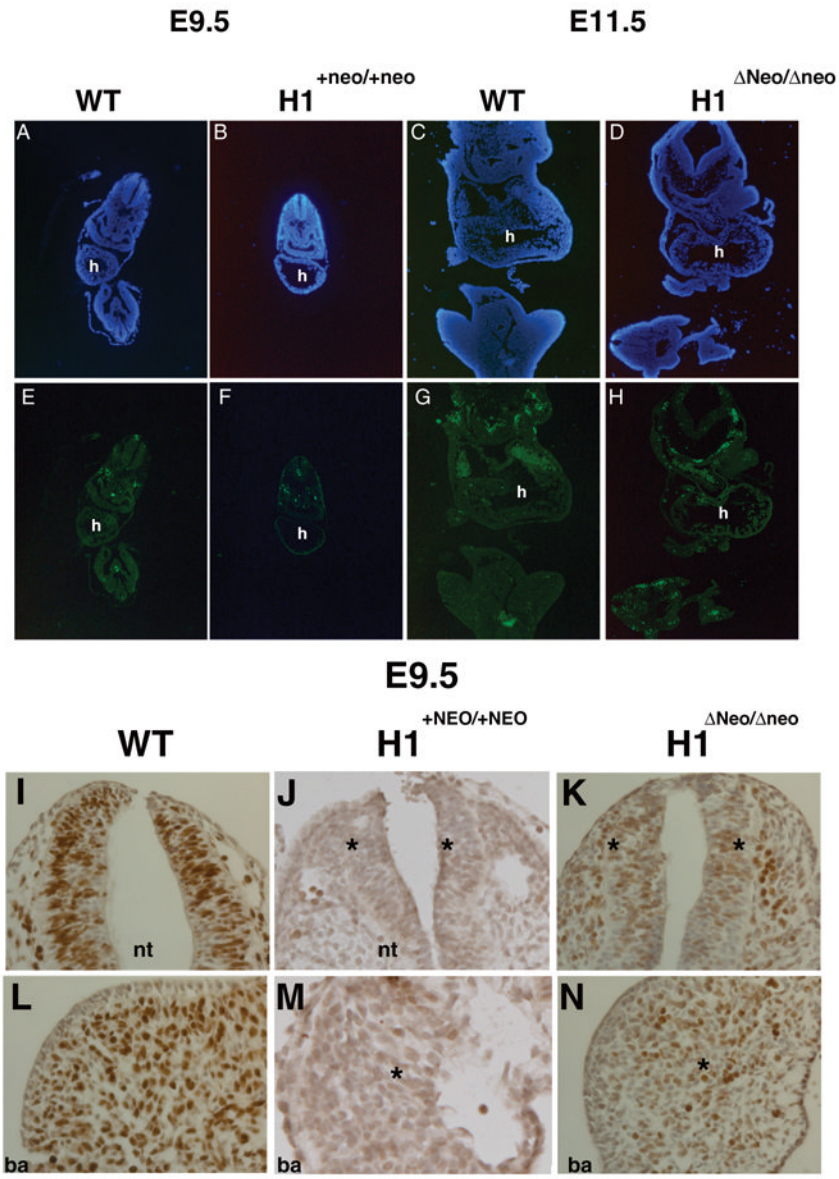

Figure 6.

(A, B, E, F) TUNEL analysis of *Hand1*$^{Hand1+Neo/Hand1+Neo}$ (E9.5) and (C, D, G, H) *Hand1*$^{Hand1\Delta Neo/Hand1\Delta Neo}$ (E11.5) embryos. Detailed comparisons show no significant difference in the level of cell death compared to wild type embryos. BrdU incorporation within wild type (I, K) and *Hand1*$^{Hand1\Delta Neo/Hand1\Delta Neo}$ E9.5 embryos. Significant decreases in cell proliferation are observed throughout mutant embryos when compared to controls. The decrease in proliferation is observed in both non-*Hand1* (neural tube I and J) and *Hand1* expressing tissues (1st branchial arch K & L). h, heart; nt, neural tube; ba, first branchial arch

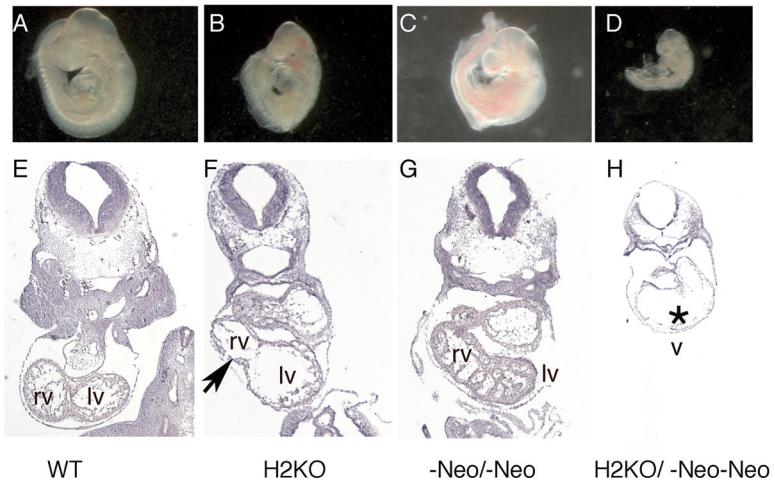

Figure 7.

Histological analysis of *Hand1*$^{Hand1\Delta Neo/Hand1\Delta Neo}$ embryos that are heterozygous and homozygous null for *Hand2* at E9.5. (A, E) Wildtype littermate; (B, F) *Hand2* null; (C, G) *Hand1*$^{Hand1\Delta Neo/Hand1\Delta Neo}$ (D, H) *Hand1*$^{Hand1\Delta Neo/Hand1\Delta Neo/}$*Hand2* null. Black arrow indicates reduced right ventricle. Asterisk indicates thin myocardium. rv, right ventricle; lv, left ventricle; v, ventricle.